

1-CAT: A MIMO DESIGN METHODOLOGY

J. R. Mitchell
J. C. Lucas

Control Dynamics Company
Office Park South
600 Boulevard South, Suite 304
Huntsville, AL 35802

ABSTRACT

The main thrust of this paper is the introduction and illustration of the One Controller at a Time (1-CAT) methodology for designing digital controllers for Large Space Structures (LSS's). In the introduction the flexible mode problem is first discussed. Next, desirable features of an LSS control system design methodology are delineated. The 1-CAT approach is presented, along with an analytical technique for carrying out the 1-CAT process. Next, 1-CAT is used to design digital controllers for the proposed Space Based Laser (SBL). Finally, the SBL design is evaluated for dynamical performance, noise rejection, and robustness.

PRECEDING PAGE BLANK NOT FILMED

INTRODUCTION

The design of attitude and vibration suppression control systems for future, large space structures (LSS's) is a difficult problem because the performance specifications are expected to be very stringent and accurate dynamical models are not anticipated before the structure is actually placed in orbit. LSS's of the future will exhibit many lightly damped flexible modes and are expected to require many actuators and sensors for adequate control authority and sensitivity. Such LSS's will comprise true, coupled multiple input, multiple output (MIMO) systems. The final design of the control system will have to be done after the structure has been tested (on orbit) and the models have been updated.

The Flexible Mode Problem

In the design of high performance attitude control systems for LSS's, flexible modes pose two distinct problems. First, they provide paths through which disturbances can be propagated throughout the structure. As a consequence, performance in attitude control can be greatly degraded. For example, in proposed high energy laser beam pointing systems, a source of disturbances will be coolant flow in mirrors used to guide the laser beam along the optical path. The effects of coolant flow on beam pointing and beam quality is modeled as disturbance signals propagating through flexible modes. The second problem is that of flexible modes being excited by command signals from the attitude control system. This is especially true in performing large angle maneuvers. For example, in a high energy laser beam pointing system, in order to change pointing directions (e.g., retargeting) a large physical element such as a mirror or a beam expander may have to be slewed. In such a

case flexible modes of the system can be significantly excited, and the settling time for the initiation of high precision pointing can become unacceptable.

Historically, the design of control systems in which flexible modes were problems has been accomplished by either attempting to gain stabilize or by notching the modes. The effects of both these are essentially the same, i.e., they tend to reduce the level that a mode can be excited, and neither approach significantly effects the modal damping in the closed loop from that of the open loop. The major drawback with gain stabilization and/or notching is that the effects of disturbances on performance is, in general, not improved and, in fact, can be worsened. Hence, gain stabilization and/or notching are only effective when disturbances are not a problem and the bandwidths of the loops are expected to be well below the first flexible mode.

In order to meet the stringent performance requirements of many LSS's it is anticipated that the control bandwidth must include a frequency range that covers the first several modes. In this case the control system must be designed so that these modes are damped, at least to the degree of the rigid body modes, and the higher frequency modes are notched or gain stabilized. Then, even though the response of the system to a standard input, such as a step, will be a multi-modal response, all the modes will decay at a minimum rate or will not be excited significantly. Modal damping is very desirable because it has a global effect over a structure, i.e., the damping of the modes will be reflected in any transfer function between arbitrary points.

Desirable Features of LSS Control System Design Methodology

Study of the digital controller design problem for Large Space Structures (LSS) has identified several objectives on which attention must be

focused when selecting a design technique. These include not only performance with respect to system behavior but also practical implementation, check-out, and operation in an orbiting space structure. The design technique desirable features are as follows:

- Simplicity of Controller

A digital controller design technique for LSS must lead to controllers of reasonable order for the very high order system models defined by flexible spacecraft. This is to minimize the computational burden of the on-board computer when the controller is implemented.

- Straightforward and Traceable Design Procedure

A design technique should be readily understandable and the design process should trace effects of closed loop control upon the system behavior throughout the design process. In this way a designer can see how the system is evolving during the design process, and therefore, have insight into problems and/or causes of problems should they arise.

- Stability of Closed Loop System

The technique should inherently provide stability of the closed loop system resulting from the combination of the digital controller and the LSS model. In fact, a reasonable amount of relative stability should be inherent.

- Inherent Robustness Checks

Robustness is of particular concern to the LSS control system designer because accurate models are not anticipated. Hence, the technique should produce designs with reasonable robustness with respect to model inaccuracies and plant variation. In addition, the design technique should provide built-in checks for robustness at stages in the design process. This is also a part of an easily traceable design procedure.

- Disturbance Rejection

Disturbance rejection is a major concern in control system design for LSS's and should inherently be achieved through the design process.

- Digital Design Accomplished in Digital Domain

Design of digital control systems should be accomplished in the digital domain so that the effects of sampling and computational transport lags can be accounted for during the design phase rather than designing a continuous controller and then attempting to implement a digital equivalent which, at best, is an approximation to the desired controller.

- Efficiency of Design

The design technique should be reasonably efficient with respect to computer processing and storage requirements and should be algorithmic in nature so that the design process can be easily repeated as model updates are obtained.

- Applicable to High Order Systems

The design technique should be capable of handling high order systems. It is anticipated that LSS models will be of order one hundred or more; hence, the numerical techniques used to implement the design methodology should be tried and proven for systems with orders in excess of one hundred.

- Incorporation of Experimental Model Data

As mentioned above, it is anticipated that the final design of an LSS cannot be completed until data from on-orbit testing is obtained. The design process should be able to easily utilize this data to generate model updates so that the control system design can be fine-tuned for increasing system performance.

Recent technological advances in the development of control system design philosophies for LSS's include Lockheed's Low Authority Control/High Authority Control (LAC/HAC),¹ TRW's Positivity,^{2,3} and General Dynamics' Model Error Sensitivity Suppression (MESS).⁴ Each of these techniques has been developed under the ACOSS Program, sponsored by the Defense Advanced Research Projects Agency (DARPA). Although the techniques take different approaches, they are common in the respect that each is carried out by following a very complex design procedure, which can even be iterative. In addition, none of these techniques possesses all the desirable features listed above.

In this paper, an alternate LSS design philosophy, called 1-CAT, is presented. When properly carried out the 1-CAT philosophy produces viable solutions to the flexible mode problem and inherently possesses the desirable features delineated above.

Theoretical Background of 1-CAT

The multi-input/multi-output (MIMO) digital controller design technique, 1-CAT, finds its basis in the fundamental principals of classical analysis and design control theory. It springs from the fact that the marriage of a MIMO system (plant) and controller can be viewed as a coupled multiloop system. The controllers for the loops cannot be designed independently, but they can be designed one at a time; this is the thesis of 1-CAT: "One Controller At a Time".

To delineate the process, consider a system having three inputs and three outputs. With all possible feedback paths open, the transfer characteristic between a particular input-output pair may be analyzed and a controller designed to stabilize the loop to satisfactory specifications. With

this loop closed, another input-output pair may be analyzed and a controller likewise designed. The second controller is not designed independently, because the effects of the first controller are taken into account when the first loop is closed. A third controller can then be designed with the first two loops closed and so on until all desired feedback paths are closed through the appropriate controller. Of course, it is doubtful that a designer would desire to close all nine possible feedback paths of this system; however, the 1-CAT technique does not preclude this possibility.

Three pertinent facts regarding the 1-CAT technique bear mention at this point.

- If the plant is stabilizable, the resulting closed loop system will be stable.

Stabilizability simply implies that if there are uncontrollable modes, i.e., modes whose eigenvalues cannot be changed by feedback, their eigenvalues must have negative real parts. In this case the uncontrollable modes cannot result in instability, but the controllable modes can. However, the 1-CAT approach can be applied so that no controllable mode can cause a stability problem and, in fact, can produce a design that will ensure a specified amount of relative stability.

For example, suppose that the 1-CAT approach is applied to a three loop example. With all loops open, assume that a controller is designed for the first loop so that all controllable modes have closed loop eigenvalues with real parts less than $-\alpha$. Now with the first loop closed a controller is designed for the second loop so that all controllable modes have closed loop eigenvalues with real parts less than $-\alpha$. Then with the first two loops closed a controller is designed for the third loop so that all controllable

modes have closed loop eigenvalues with real parts less than $-\alpha$. Now suppose a root locus study is performed on the first loop with the second and third loops closed and with the controllers designed for each loop included. The controllable modes in this loop can be separated into those modes only controllable from loop one and those modes that are also controllable from loops two and/or three. Using the gain factor for which loop one was designed, those modes only controllable from loop one must have eigenvalues with real parts less than $-\alpha$, since these modes are not affected by the designs in loop two and/or three and loop one was designed to achieve this specification. The other controllable modes in loop one must have eigenvalues with real parts less than $-\alpha$ since these eigenvalues are controllable from loop two and/or three which were also designed to meet this specification.

The bottom line is that as subsequent loop closures are made eigenvalues of preceding loops cannot have real parts greater than $-\alpha$. However, it should be noted that if a subsequent loop is designed with a more relaxed specification, the relative stability of the preceding loops can relax, too.

Although the above arguments have been made for the first loop of a three loop example, they obviously can be extended to the design of a system with many loops and to other loops rather than the first. In addition, other measurements of relative stability can be used, e.g., gain margins and phase margins. In order to ensure no degradation in the relative stability of loops previously closed, subsequent loops should be designed so that relative stability is improved or at a minimum not allowed to degrade.

Implementation of the 1-CAT Philosophy

If carried-out properly, the 1-CAT philosophy is a sound approach for designing MIMO control systems. It is obvious that, at least from a

theoretical point of view, root locus techniques could be used to carry out the design process. However, this would require transfer functions of all the elements of the transfer function matrix. Since LSS's are anticipated to be high order, e.g., one hundred or more, these transfer functions will be difficult to obtain and cumbersome to handle with root locus techniques.

An alternative approach is frequency response techniques. One frequency response approach that could be used, is one in which the frequency response data is generated along the line $-\alpha + j\omega$, where α is the stability margin in which it is desirable that all poles be to the left. Then as loops are closed, all those modes lying to the right of the $-\alpha$ line are forced to produce counter clockwise encirclements of the $-1.0 + j0.0$ point on the Nyquist plot. When the design is completed, the compensation can be easily frequency shifted, back to $\alpha = 0$. This is a theoretically sound approach; however, it does not easily accommodate experimental data, since frequency response data along the line $-\alpha + j\omega$ is difficult to generate experimentally or to compute from experimental results.

Another frequency domain approach is to use classical frequency response data, i.e., $\alpha = 0$ data, and design each loop to specified gain margins, phase margins, etc. There are two questions that must be answered in regard to this approach:

- (1) How can these designs be achieved, and added modal damping be assured?
- (2) As subsequent loops are closed, how can degradation in the performance of the closure of previously closed loops be avoided?

The answer to the first question is that modal damping can be added to flexible modes by properly phase stabilizing the modes. Phase stabilization

of a mode is achieved by designing compensation so that on an open loop polar frequency response, the peak of the mode occurs when the phase is near 0° .

The amount of damping added to a mode is a function of the amount of peaking of the mode. From root locus techniques it is well known that when a loop is closed and the loop gain factor is increased, the poles migrate from the open loop pole locations toward the open loop zero locations. Interpreting this in terms of phase stabilization means that the higher a phase stabilized mode is made to peak in the open loop, the closure it will approach a left-half plane open loop zero in the closed loop. If the zero is well in the left half plane, significant damping to the mode can be added with significant modal peaking. If the damping of the zero is small, e.g., it may even be less than that of the pole, there are two routes that can be taken. First, compensation can be designed that has a pole that migrates to the zero with small damping. The compensation zero can be selected further in the left half plane with an acceptable damping. Then, the mode can be forced to have significant peaking and consequently approach the damping of the compensation zero.

The second route is to design for maximum modal damping. It is a fact that when a mode is phase stabilized and the loop gain is increased, its initial break is into the left half plane. However, if the peaking is increased, the damping can reach a maximum value and then decrease. Such a case occurs when the zero, toward which the mode is migrating, has damping on the same order or less than the corresponding mode. For lightly damped modes, such as occur in LSS's, this is indicated on an open loop frequency response plots by deep troughs in the magnitude characteristics. For such

situations, maximum damping can be approximately achieved by phase stabilizing the mode and selecting the loop gain so that the peak of the mode is above 0 dB and the trough of the zero, toward which the mode is migrating, is below 0 dB. If several modes are to be handled in this fashion, then frequency shaping of the loop gain will be required so that each mode satisfies this condition.

Now returning to the second question. In order that subsequent loop closures will not degrade the open loop performance of previous closed loops, the dominant frequency ranges of modes controlled in previous loops, i.e., designed for increased damping, must be precluded from the interior of the unit disk centered at $-1 + j0$ point in the $GH(j\omega)$ - plane for each subsequent loop closure. In essence this means that if a dominant mode of a previously closed loop is dominant in a subsequent loop it must still be phase stabilized to assure that damping is not lost. It should be noted that rigid body modes are included here.

Loop Closure in MIMO Systems

The 1-CAT design philosophy dictates that feedback loops are sequentially designed and closed. A frequency response approach was selected because either continuous or sampled-data frequency responses are numerically easy to compute (even for high order systems) and frequency response data are easily obtained from experimental results. By following the rules of the previous section degradation in loop performance by subsequent loop closures can be assured. In this section, an analytical technique for taking into account a loop closure in a MIMO system is presented. It should be noted that the presentation is made using continuous transfer function notation but

interpretation in terms of standard frequency responses or sampled-data frequency responses simply requires a change in the function notation; hence, no generality is lost.

A block diagram representation of a multiple input, multiple output (MIMO) system is shown in Figure 1. One approach for mathematically representing this is through the transfer function matrix, i.e.,

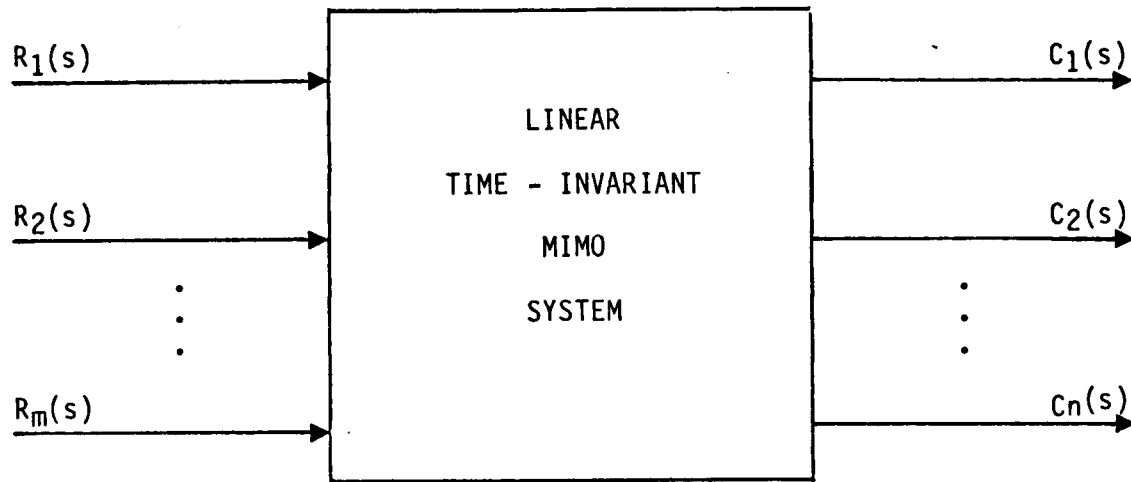


Figure 1. Block Diagram of a MIMO System.

$$[G(s)] = \begin{bmatrix} G_{11}(s) & G_{12}(s) & \dots & G_{1m}(s) \\ G_{21}(s) & G_{22}(s) & \dots & G_{2m}(s) \\ \vdots & \vdots & & \vdots \\ G_{n1}(s) & G_{n2}(s) & \dots & G_{nm}(s) \end{bmatrix} \quad (1)$$

in which

$$\frac{C_i(s)}{R_j(s)} = G_{ij}(s). \quad (2)$$

The transfer function matrix description given by (1) can be used to represent either closed loop or open loop systems. All that is required is that when a loop is closed the matrix must be recomputed to reflect the loop closure.

In fact, the computation of the elements of the matrix can be done in a straight forward manner. A loop closure from output p to input k through a feedback compensator $K_2(s)$ and forward path compensator $K_1(s)$ is shown in Figure 2. This system can be represented in the form of Figure 1 by recomputing the elements of the new system matrix as follows:

$$G'_{ij}(s) = G_{ij}(s) - \frac{K_1(s) K_2(s) G_{ik}(s) G_{pj}(s)}{1 + K_1(s) K_2(s) G_{pk}(s)}, \quad \begin{matrix} i \neq p \\ j \neq k \end{matrix} \quad (3)$$

$$G'_{pj}(s) = \frac{G_{pj}(s)}{1 + K_1(s) K_2(s) G_{pk}(s)}, \quad j \neq k, \quad (4)$$

$$G'_{ik}(s) = \frac{K_1(s) G_{ik}(s)}{1 + K_1(s) K_2(s) G_{pk}(s)}, \quad (5)$$

where $i = 1, 2, \dots, n$ and $j = 1, 2, \dots, m$ and the prime notation represents the elements of the new matrix. In summary, equation (3) is used to compute all the elements of the matrix except those in the p^{th} row and k^{th} column; equation (4) is used to compute all the elements in the p^{th} row except the k^{th} element; equation (5) is used to compute the elements of the k^{th} column.

By investigating the frequency responses of equations (3), (4) and (5) several observations on closing loops in MIMO systems can be made. First, from (4) it is seen that in the frequency range where $|1 + K_1 K_2 G_{pk}(j\omega)|$ is larger than unity the p^{th} output becomes less affected by all inputs except $R_k(s)$. The implications are that as loops are closed, the p^{th} output tends

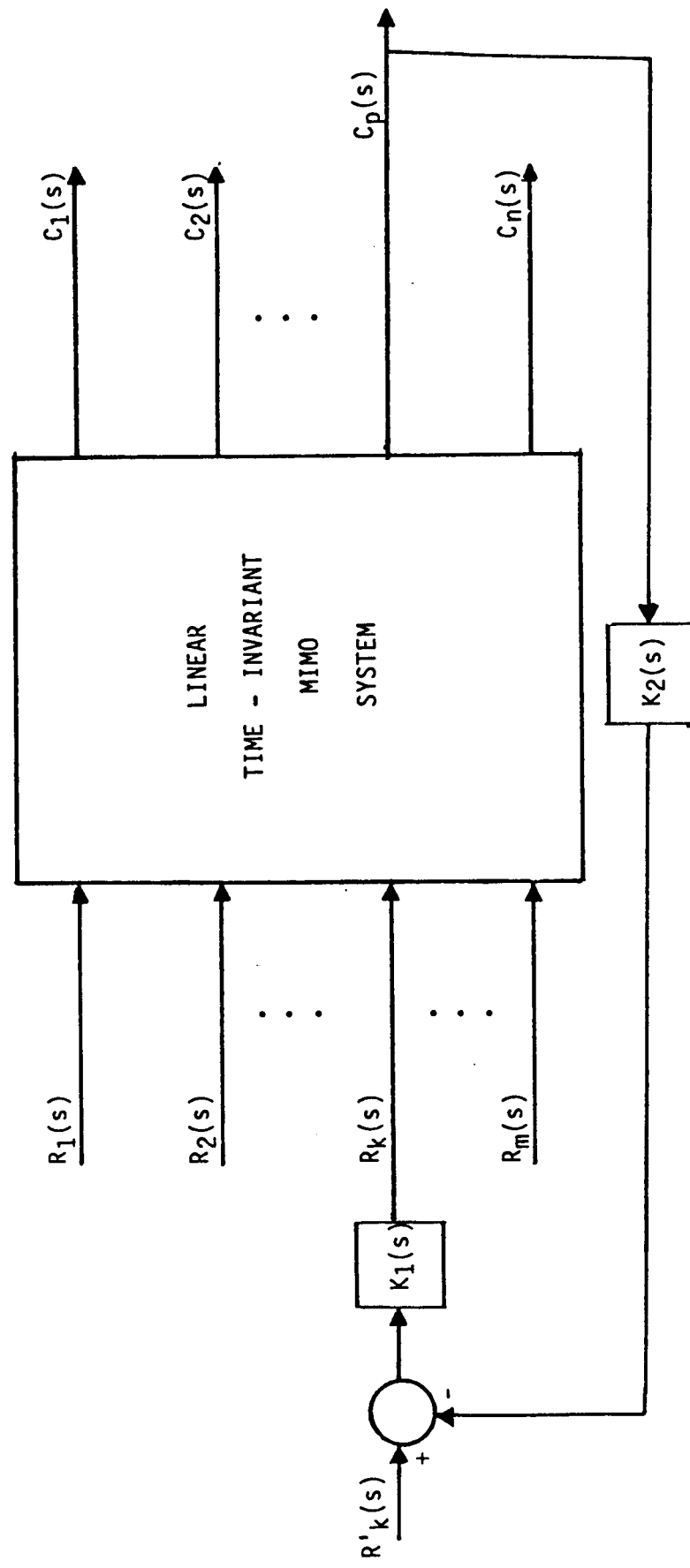


Figure 2. MIMO System with Feedback from Output p to Input k .

to be decoupled from the other inputs in the frequency range where $|K_1 K_2 G_{pk}(j\omega)| \gg 1$, which is roughly the control frequency range. In fact, if in the control frequency range the product of the compensators $K_1(j\omega) K_2(j\omega)$ is selected so that the polar frequency response of $K_1 K_2 G_{pk}(j\omega)$ does not violate the unity disk centered at $-1.0 + j0.0$ in the $K_1 K_2 G_{pk}(j\omega)$ plane decoupling from the other inputs over the whole control frequency range is assured. The amount of decoupling on a frequency by frequency basis is easily seen by reviewing the amount that the frequency response of $|1 + K_1 K_2 G_{pk}(j\omega)|$ is above 0 dB.

In the cases where loops are closed with a unity forward transfer function, e.g., vibration suppression loops for LSS's, a decoupling effect over the control frequency range is not only realized between the other inputs and the p^{th} output but between the k^{th} input and the other outputs. Investigating equation (4) in a similar fashion as done for (3) above easily validates this statement.

Another observation from equation (3) is that by closing a loop between the k^{th} input and p^{th} output the transmission zeros between the other inputs and other outputs are affected. In fact, from (3) a designer can see exactly what the product $K_1 K_2$ needs to be in order to place zeros in desirable locations. For example, to generate a notch at $\omega = \omega_1$ in $G_{ij}(s)$ where $i \neq p$ and $j \neq k$, then

$$K_1 K_2 (j\omega_1) = \frac{-G_{ij}(j\omega_1)}{G_{ij}(j\omega_1)G_{pk}(j\omega_1) - G_{ik}(j\omega_1)G_{pj}(j\omega_1)} \quad (6)$$

With the frequency response of the elements of the transfer function matrix available, a designer can easily carry-out the 1-CAT process by

sequentially using equations (3), (4), and (5). A check on the effects of a loop closure on any element of the transfer matrix can be made by simply comparing "before" and "after" frequency responses. System robustness can be determined by opening individual loops, with the other loops closed, and looking at closest approach points to the $-1.0 + j0.0$ point.

Design of Space Based Laser Attitude Control System Using 1-CAT

In order to demonstrate the application of 1-CAT on a reasonable order LSS control problem, an attitude and vibration suppression control system is designed for a planar model of the Space Based Laser (SBL). Figure 3 shows the structural model of the SBL. As indicated by the figure the structure containing the mirrors is attached to ground through an isolator. While in reality the mirror structure is actually attached to the Aft section of the orbiting platform, the approximation is reasonable for the differences in mass of the two sections.

The goal is to design a beam tilt angle control system with acceptable dynamic performance and disturbance rejection. The tilt angle of the beam can be controlled by torquing the primary support structure of the beam expander about its gimbal point, assumed centered at the connection of the isolation system and the beam expander, by torquing the secondary mirror (SM), and by independently torquing any or all of the primary mirror segments (PM1, PM2, PM3). The secondary mirror angular rate is sensed inertially, whereas the angular rate of each segment of the primary mirror is sensed relative to the primary support structure. The tilt angular error is sensed in inertial space by the Outgoing Wavefront Sensor (OWS).

Table 1 and 2 contain the data used in constructing the model of the SBL. Included in this model are twenty-six degrees of freedom containing many flexible modes which are insignificant to the design effort. Modal truncation can be used to reduce the order of the system in order that (1) unnecessary calculations are eliminated and (2) some significant modes be eliminated so post analysis can establish the effects of unmodeled modes on

TABLE 1. OSBL MODAL DATA

Modal frequencies Hertz	Tilt error gains	Gimbal point inertial rotation gain		1st Segment of the primary mirror gain	2nd Segment of the primary mirror gain
		1	2		
1	0.0	0.0	0.1420E-02	0.1000E-02	0.0000E+00
2	0.0	0.0	-0.0000E+00	0.0000E+00	0.0000E+00
3	0.0	0.0	-0.3724E-03	-0.4694E-03	0.0000E+00
4	4.471117	28.10601	0.1774E-01	0.6057E-03	0.2104E-03
5	6.592096	41.42439	-0.5440E-07	-0.1499E-08	-0.5427E-07
6	7.061209	44.36600	0.1300E-00	0.1922E-09	0.2104E-09
7	7.414550	46.50699	-0.1050E-01	-0.1000E-02	-0.1450E-02
8	9.251712	50.13035	-0.6090E-04	0.7359E-05	-0.0577E-02
9	9.252620	50.13593	-0.3199E-05	0.5666E-07	0.2726E-04
10	9.530362	59.00103	0.2332E-01	-0.1039E-03	0.1200E-01
11	9.001935	62.03903	-0.3419E-02	0.3032E-04	-0.3277E-03
12	9.997501	62.01615	-0.3124E-07	-0.2670E-10	-0.1446E-07
13	10.00001	62.81193	-0.1301E-07	0.1244E-09	-0.0045E-08
14	10.46396	65.74702	0.2377E-01	0.4017E-04	0.2110E-01
15	10.80504	67.09510	-0.2290E-06	0.3015E-05	-0.9200E-02
16	10.00673	67.90071	0.4044E-05	-0.2000E-07	0.1594E-01
17	11.94206	75.03420	0.2414E-02	0.1432E-02	-0.3779E-02
18	12.85439	80.76653	0.1455E-00	0.4536E-09	-0.2093E-04
19	15.49192	97.35114	-0.0032E-02	0.2171E-03	-0.2495E-02
20	17.50351	109.9770	0.5707E-02	0.1370E-02	-0.3002E-02
21	17.94535	112.7510	-0.7000E-09	-0.3152E-09	0.1692E-04
22	23.47099	147.5228	-0.2010E-01	0.1405E-02	-0.5573E-02
23	29.26876	181.9010	0.2309E-10	-0.5097E-11	0.3235E-11
24	77.00790	404.3576	-0.1010E-00	0.3061E-09	-0.2495E-02
25	89.34500	561.3762	-0.6393E-02	0.5100E-02	-0.5641E-02
26	145.0540	911.4013	-0.2000E+00	-0.1416E-03	0.1422E-03

**ORIGINAL PAGE IS
OF POOR QUALITY**

TABLE 1. OSBL MODAL DATA (continued)

Modal frequencies Hertz	Modal frequencies RAD/SEC	Jrd Segment of the primary mirror gain	Secondary mirror inertial rotational gain	Gimbal point inertial Y		Secondary mirror inertial Y translation gain
				C	S	
1	0.0	0.0	0.0000E+00	0.1000E-02	0.0000E+00	0.2524E-01
2	0.0	0.0	0.0000E+00	0.0000E+00	0.0000E+00	0.0000E+00
3	0.0	0.0	0.0000E+00	-0.1694E-03	0.1034E-01	0.3757E-02
4	4.47337	20.10601	-0.2390E-03	-0.4000E-01	0.7600E-03	0.5439E-03
5	6.592096	41.42439	-0.7709E-07	0.7500E-07	-0.3709E-00	-0.5502E-00
6	7.061209	41.36600	-0.5392E-05	-0.2026E-00	-0.1636E-09	0.1491E-00
7	7.414550	46.50699	-0.1410E-02	0.1566E-01	0.0142E-03	-0.1260E-01
8	9.251732	50.13035	-0.0513E-02	0.1461E-03	0.1790E-05	-0.1404E-03
9	9.252620	50.13593	-0.1401E-01	-0.5420E-06	0.1108E-06	0.5019E-06
10	9.530362	59.00103	0.1208E-01	0.3111E-02	-0.9761E-03	-0.3107E-02
11	9.8001935	62.09003	-0.3276E-03	0.03711E-02	0.3223E-04	-0.0530E-02
12	9.997501	62.01615	-0.7564E-05	-0.5596E-06	0.1276E-00	0.6074E-00
13	10.00001	62.01193	-0.8074E-08	0.2265E-09	-0.1624E-09	-0.1340E-09
14	10.46396	65.74702	0.1210E-01	0.4413E-03	-0.1211E-02	-0.4615E-03
15	10.80504	67.09510	-0.9144E-02	0.1797E-03	-0.4270E-05	-0.1062E-03
16	10.80673	67.90071	-0.1597E-01	0.2110E-05	-0.1055E-06	-0.2015E-05
17	11.94206	75.03420	-0.3779E-02	-0.2110E-01	0.4751E-03	0.2322E-01
18	12.85439	80.76653	0.2093E-04	-0.7007E-00	0.1600E-09	-0.0121E-08
19	15.49392	97.35114	-0.2314E-02	0.1250E-01	-0.1054E-01	-0.1410E-01
20	17.50351	109.9778	-0.3002E-02	-0.2626E-01	-0.7049E-02	0.3105E-01
21	17.94535	112.7540	-0.1691E-04	0.1433E-00	-0.5101E-08	-0.1025E-00
22	23.41899	147.5228	-0.1573E-02	0.0570E-01	-0.1631E-03	-0.1199E-09
23	29.26076	183.9010	0.2407E-04	-0.1217E-09	-0.3312E-11	-0.2961E-09
24	77.01790	404.3576	0.2495E-02	0.3040E-09	0.3206E-02	0.2508E-02
25	89.35500	561.3162	0.2331E-02	-0.1501E-01	-0.7452E-04	0.1444E-01
26	145.0540	911.4013	0.7271E+00			

TABLE 2
 ACTUATOR AND SENSOR DYNAMICS
 GIMBAL TORQUE ACTUATORS

$$G_{GT}(s) = \frac{(200)^2}{s^2 + 2(.707)200 s + (200)^2}$$

TILT ANGLE SENSOR

$$G_{TA}(s) = \frac{125}{s + 125}$$

MINOR ACTUATORS

$$G_{SM}(s) = \frac{500}{s + 500}$$

RATE SENSORS

$$G_{RS}(s) = \frac{250s}{s + 250}$$

ISOLATOR

$$I(s) = 628.3s + 3948$$

the final design. It should be noted that modal truncation is not a prerequisite for the application of 1-CAT. By using the frequency response techniques mentioned earlier model order does not pose a significant constraint on the design process.

Modal truncation is easily accomplished in the frequency domain by examining the relative peaking of each mode. A step-by-step process of modal selection can be achieved by examining the DC gain and resonant peak gain of each mode. The gains defined by the relations in equation 7 and 8 provide a basis of comparison between each flexible mode and the rigid body modes.

$$\text{DC GAIN} = \frac{G_{pi} T_{ai}}{\omega_i^2} \quad (7)$$

$$\text{RESONANT PEAK GAIN} = \frac{G_{pi} T_{ai}}{2\zeta \omega_i^2} \quad (8)$$

where

G_{pi} is the gimbal point torque modal gain at the i-th mode

T_{ai} is the tilt angle angular sensor modal gain at the i-th mode

ω_i is the i-th modal frequency.

The process begins by computing the rigid body gain at each flexible modal frequency. This gain is compared to the DC gain for the particular mode of interest. The largest DC gain that exceeds both the rigid body gain for that frequency and all other modal DC gains is labeled a dominant mode, W_{d1} . The process continues with the dominant mode W_{d1} replacing the rigid body modes as a basis of comparison. The DC gain of each mode lying at a

higher frequency than W_{d1} is compared to the gain of the mode W_{d1} at each succeeding mode frequency. If a mode's DC gain dominates the gain of the mode W_{d1} at that frequency W_i and is larger than all other remaining DC gains then it is chosen as W_{d2} . This process continues until all modes have been compared in this fashion. The resulting selection would appear somewhat as the solid line of Figure 4. This solid line is actually the straight line approximation of the magnitude frequency response. Once this has been achieved, the selection criterion proceeds to check the resonant peak of each mode defined by (8). If the resonant gain is such that it exceeds the value of the straight line approximation at that mode frequency W_i then it can be included in the model. This step must be tempered with practicality since the resonant peak may exceed the curve with a only small value of epsilon. Technically its effects are noticeable but it is inconsequential to the design. A reasonable and easily implemented solution is to choose only those modes whose resonant gain exceeds the DC gain curve by a tolerance which is defined by the designer.

Relations (7) and (8) were applied to the modal data in Table 1 with the resulting selection of modes being listed in Table 3. Modes 25 and 26 are ignored for this design even though they would have been considered by this process. The validity of modes at frequencies this high is questionable.

In addition to the dynamics of the modes presented in Table 1, sensor and actuator dynamics were included in the model in order that the design problem be more realistic. The bandwidth for all sensors and actuators except for the tilt angle sensor is just outside the range of the modal frequencies selected for the model. This provides a phase shift in the modal frequency range without gaining any gain stabiliziton from the actuator and sensor dynamics.

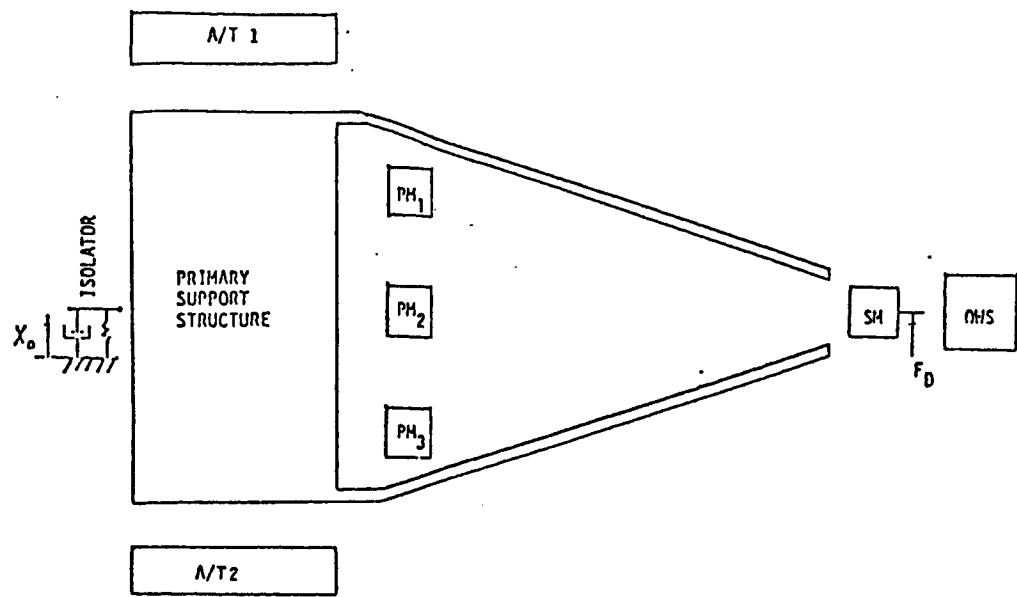


Figure 3. SBL Beam Expander Structural Model.

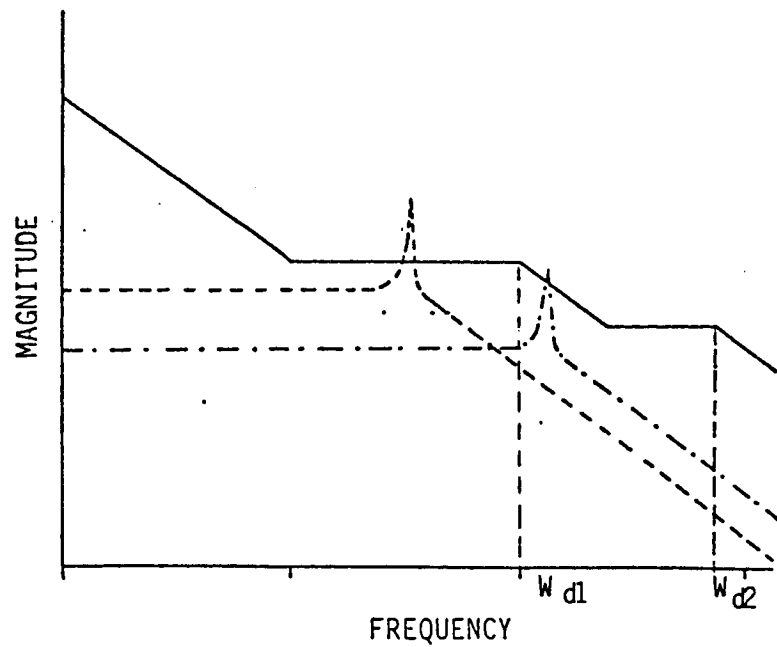


Figure 4. Modal Selection Criterion

TABLE 3
SELECTED MODES AND FREQUENCIES

Mode No.	Frequency rad/sec
1	0
3	0
4	28.10681
7	46.58699
10	59.88103
14	65.74702
17	75.0342
19	97.35114
20	109.9778
22	147.5228

Since the isolation system is assumed attached to ground, it provides a path for AFT disturbances to be propagated to the tilt error. This is illustrated in the system model shown in Figure 5. In this figure \underline{K}_{pm1} , \underline{K}_{pm2} , \underline{K}_{pm3} , \underline{K}_{sm} , and \underline{K}_g are, respectively, the torque modal gain vectors of the three primary mirror segments, the secondary mirror and the gimbal. K_i is a disturbance force error modal gain vector, \underline{l}_T^T is the transpose of the tilt angle modal gain vector, and \underline{l}_I^T is the transpose of the modal displacement vector at the gimbal point. The other modal gain vectors denoted by the symbol \underline{l} with the appropriate subscripts are the sensor modal gain vectors at the designated structural points. The transfer function matrix $G(s)$ is the modal transfer function previously defined. $I(s)$ represents the isolator whose transfer function is listed in Table 2.

The design problem for the SBL can now be restated as the determination of a digital feedback control law for commanding torques at the secondary mirror, the gimbal, and each segment of the primary mirror so that: (1) commanded tilt angle is accurately achievable with a reasonable dynamic response and (2) disturbances have minimum effect on tilt angle.

SBL Control Law Design and Analysis

Figure 6 shows the digital feedback control law selected to accomplish the goals of the design. The basic operation is that of closing a negative feedback path around each mirror by sampling the sensed rate of each mirror and operating on the signal with a digital controller to obtain a commanded torque signal which is converted to an analog signal for each mirror actuator.

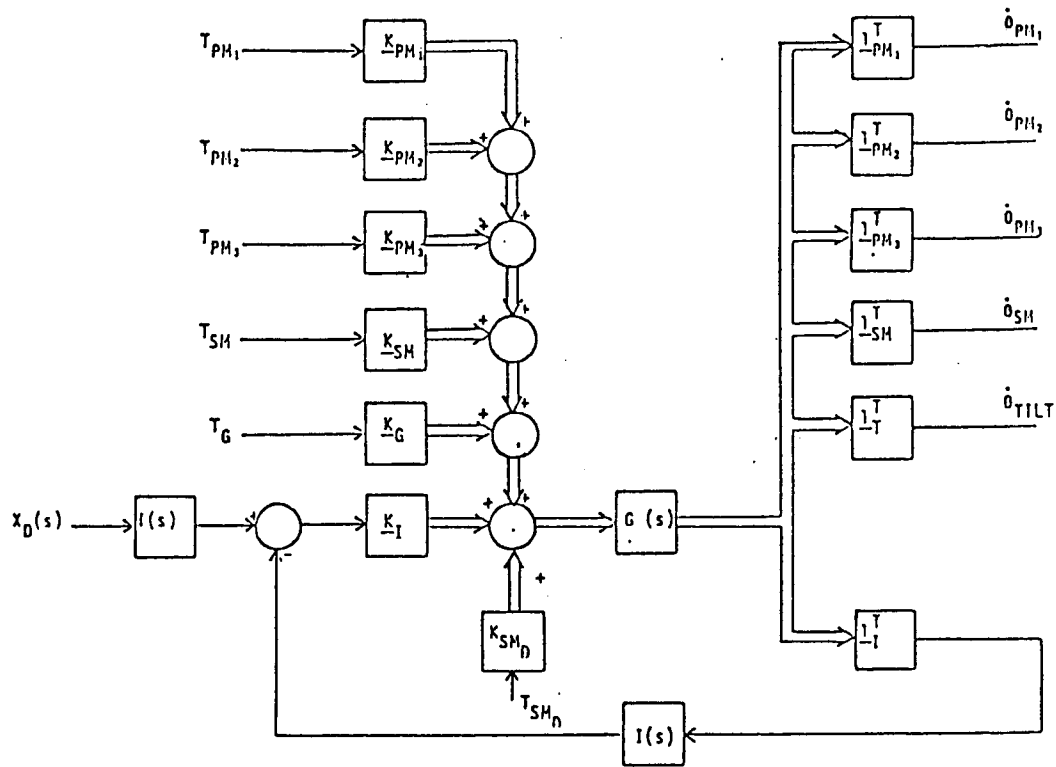


Figure 5. Vector-matrix block diagram showing the feedback path around the system dynamics due to the isolation system.

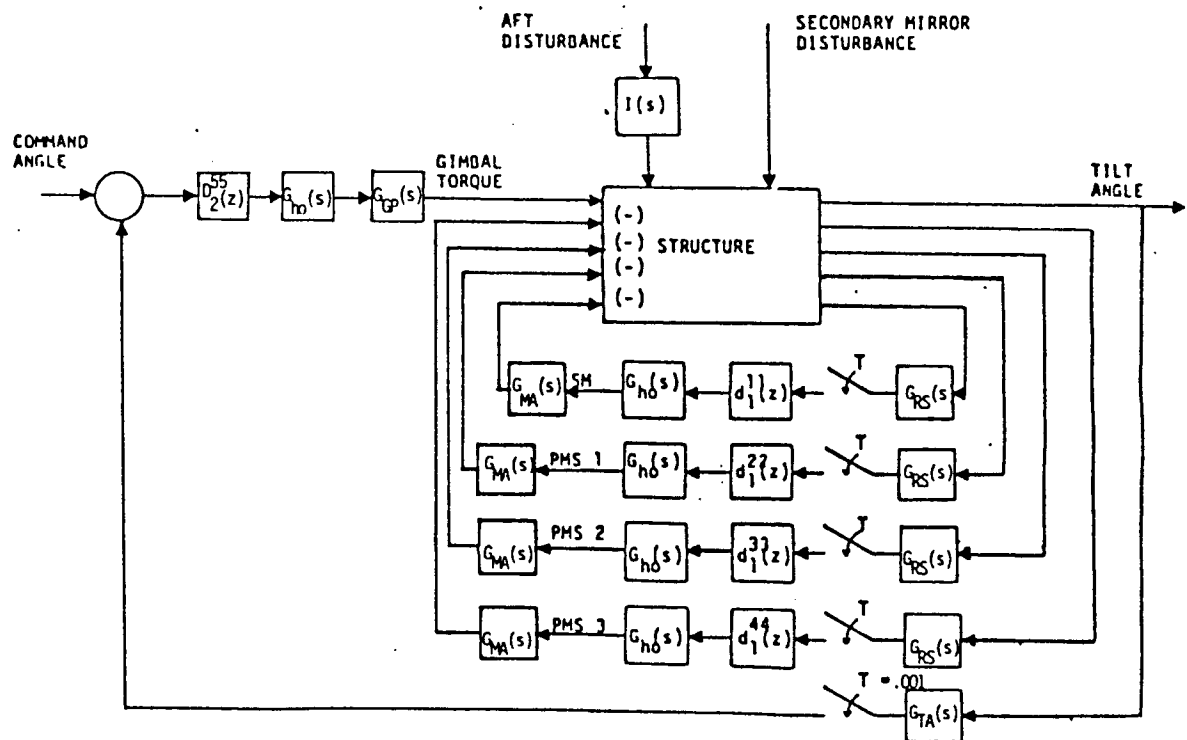


Figure 6. Block Diagram For OSBL

The effect of closing the loops is to obtain damping in the tilt angle loop. The negative sign in the block labeled STRUCTURE indicates the differencing to obtain an error signal. For these rate loops the desired rate is always zero; hence, the error signal is simply the negated value of the each digital controller. Similarly a negative feedback loop is formed for the attitude signal by differencing the commanded angle with the sampled value of the sensed tilt angle and then operating on the error with a digital controller in the forward path. The digital controller is placed in the forward path to insure zero steady state error as well as closed loop stability. The block labeled STRUCTURE is essentially the block diagram shown in Figure 5 with the exception of the minus sign discussed earlier. Each loop is to be design with as high a bandwidth as possible, which for this particular design implies that the digital controllers should be designed with as high a gain as possible. This will insure disturbance rejection as well as achieved the dynamic response required.

The 1-CAT approach can be readily applied to this designed. The order in which the loops are closed will be first the secondary mirror loop, the three primary mirror segment loops in numerical order, and then the tilt angle loop.

In order to better see the effects of the design and the closure of each loop on the tilt angle loop, the open loop frequency responses of the SM, PM1, PM2, and Tilt angle loops are shown in Figures 7-10. The frequency response of PM3 has been ignored because it like the response of the PM2 loop is very much the same as the response of PM1. This is due to the structure of the SBL being primarily symmetric about the line of sight. The response of the Tilt angle loop shows very clearly eight flexible modes. The dynamical

effect occurring at .6 rad/sec is due to the isolation system. The response of the SM loop indicates that six flexible modes of the model are significant in this loop while the responses of PM1 and PM2 indicate that only two modes show a large dynamical response in the two rate loops.

As stated earlier the design begins with the secondary mirror loop, and on close examination of the frequency response of the loop, the modes are found to be near perfectly phase stabilized. With this in mind, the loop is closed with a simple gain factor of 70 dB. This produces a gain margin of 22 dB with a phase margin of 40 degrees. Closing this loop with a gain factor of this magnitude will produce naturally tracking notches in the remaining loops at the frequencies of the dominant modes of this loop.[5] The resulting tilt angle loop response with the SM loop closed is shown in Figure 11. By comparing Figure 11 to Figure 10, the effects of the loop closure are obvious. Each mode that was phase stabilized and amplified in the SM loop is reduced in the tilt angle loop. In addition, by comparing the phases for each mode it is seen that the modes have been damped. The primary mirror segment loops were not appreciably affected since neither of the dominant modes of those loops are significant in the secondary mirror loop.

With the secondary mirror loop closed, the design proceeds with the first primary mirror segment loop in a similar manner. Close examination of the PM1 frequency response with the SM loop closed indicates the dominant modes to be near perfectly phase stabilized, however, the other flexible modes present are not phase stabilized and adding gain to these modes will result in the lowering of the damping of those modes in other loops containing modes of similar frequencies. A gain factor of 100 dB is chosen for compensation in this loop since dynamical compensation for the other modes would

not significantly enhance the design due to their low gain. The resulting gain margin is 24 dB. The results of the loop closure is very evident in the remaining primary mirror loops as well as the tilt angle loop. The dominant modes of PM1 have been completely eliminated in the remaining open loops as indicated by Figures 12 and 13. The damping of the flexible mode at 75 rad/sec has been decreased due to slightly too much gain in PM1, but comparison to Figure 11 shows that the overall response is now improved. Due to the similarity of the primary mirror loops nothing is to be gained by changing the design of 100 dB, and hence those loops are closed with 100 dB gain factors and similar gain margins results.

The effects of the closing of the rate loops on the tilt angle loop are easily seen by comparing Figures 10 and 14. The tilt angle loop now has the low frequency phase approaching from -90 degrees as opposed to it approaching from -180 degrees. In addition, the flexible modes have been damped by the rate loops automatically increasing the bandwidth. These improvements greatly aid in achieving a reasonable closed loop bandwidth and dynamic response for the tilt angle loop. The compensators used to achieve a high bandwidth and reasonable stability margins are listed as follows:

Gain Factor of 130 dB

First Order Lead Compensator that produces 55 degrees at 7 rad/sec.

$$D_1(z) = \frac{9.9595566 z - 9.937599}{z - .09789425}$$

Second Order Dominant Pole Compensator with a break frequency of 11.3 rad/sec and a damping ratio of .1.

$$D_2(z) = \frac{3.19262 z^2 + 6.38524 z + 3.19262}{10000(1.00116 z^2 - 1.99994 z + .9989)}$$

First Order Lag Compensator that produces -10 dB and -30 degrees at 200 rad/sec.

$$D_3(z) = \frac{.2556939 z - .2129331}{z - .9572393}$$

The compensated open loop tilt angle frequency response is shown in Figure 15. The stability margins of this response are

$$\text{phase margin} = 41 \text{ degrees}$$

$$\text{gain margin} = 12 \text{ dB.}$$

A closed loop frequency response of the tilt angle loop with all other loops closed is shown in Figure 16. From this plot of the response, the closed loop bandwidth is found to be 1.3 Hz. The resonant peak of the response is 3.9 dB occurring at .52 Hz, and no flexible modal peak is greater than -10 db.

Figures 17 and 18 show the frequency response of the secondary mirror loop and the first primary mirror segment loop respectively. Each response shown is an open loop response with all other loops closed. The purpose of this action is to examine the stability margins of each loop with all other loops closed. The original stability margin of the secondary mirror loop was a gain margin of 22 dB and a phase margin of 40 degrees. The original margins are relatively unchanged but an additional gain margin of 15 dB is now added due to the cancelation of the rigid body response in the loop. The first primary mirror loop has a gain margin that is relatively unchanged from its original value as well as the other two primary mirror rate loops.

Figure 21 shows the results of a step response of the SBL tilt angle control system. The response is clearly dominated by a pair of complex conjugate poles with an undamped natural frequency of approximately .5 Hz (as is suggested by the frequency domain analysis). The percent overshoot is approximately 48% while the settling time is 2.3 seconds.

In addition to a reasonable dynamical response, it is desirable to have a robust design. Figures 19 and 20 indicate that the design is indeed robust. Figure 19 is an open loop response of the tilt angle loop with the first two flexible modes reduced in frequency by 20%. The gain margin and phase margin are now 3 dB and 42 degrees respectively. Although the gain margin is reduced, the system is still closed loop stable. The closed loop response of the tilt angle loop shows an unchanged bandwidth and resonant peak with a modal peak of 7 dB.

A step response of this perturbed model is shown in Figure 22. The response clearly shows the undamped pair of complex conjugate poles at 15 rad/sec. Although the step response has a high frequency component added to it, both pair of poles "die" out at approximately the same rate. The percent overshoot has increased to 75% while the settling time has remained relatively unchanged.

Disturbance rejection is a requirement of the SBL design for the line of sight or tilt angle. Figures 23 and 24 show the open and closed loop for both an aft disturbance and secondary mirror coolant disturbance respectively. The closed loop response is reduced in comparison to the open loop response in both figures and indicates good disturbance rejection by the designed system.

In addition, the disturbance rejection properties of the system is illustrated by the application of the Aft Disturbance PSD of Figure 25 and the Coolant Disturbance PSD of Figure 27. Again it is seen by Figures 26 and 28 that the closed loop response shows a marked improvement over the open loop response of the tilt angle loop.

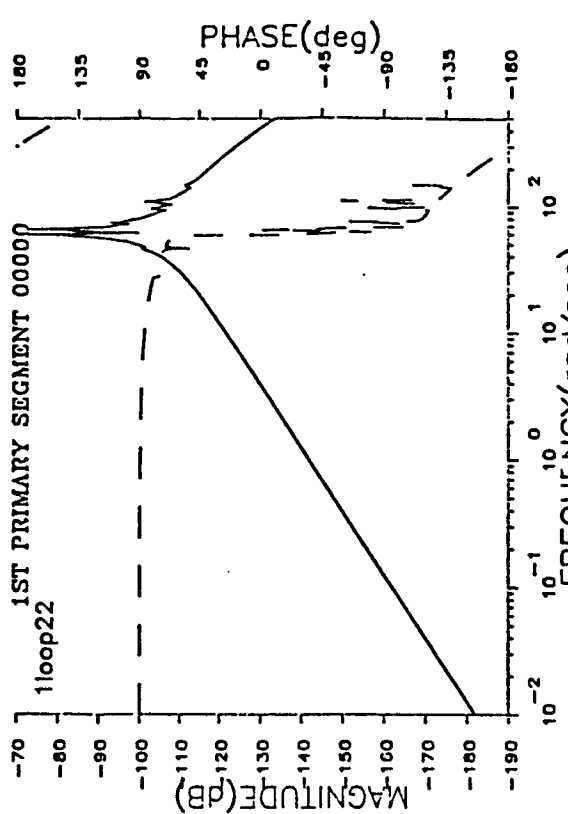


Figure 8. 1st Primary Mirror Rate (rad/sec)/1st Primary Mirror Applied Torque (N-m) all Feedback Paths Open.

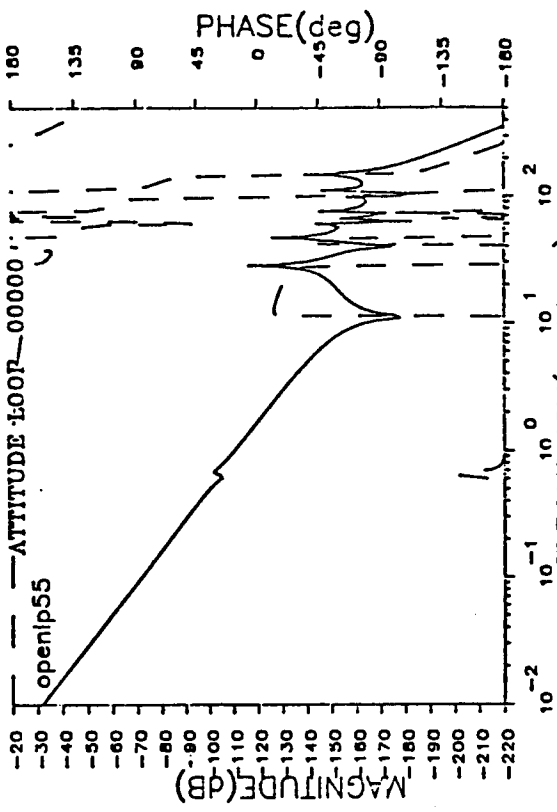


Figure 10. Tilt Angle (Rad)/Gimbal Point Torque (N-m). all Feedback Paths Open.

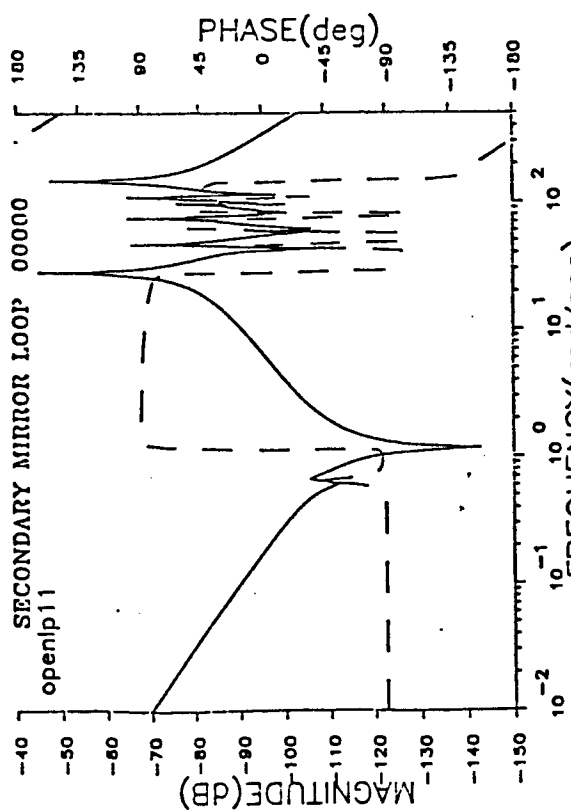


Figure 7. Secondary Mirror Angular Rate (rad/sec)/Secondary Mirror Applied Torque (N-m) all Feedback Paths Open.

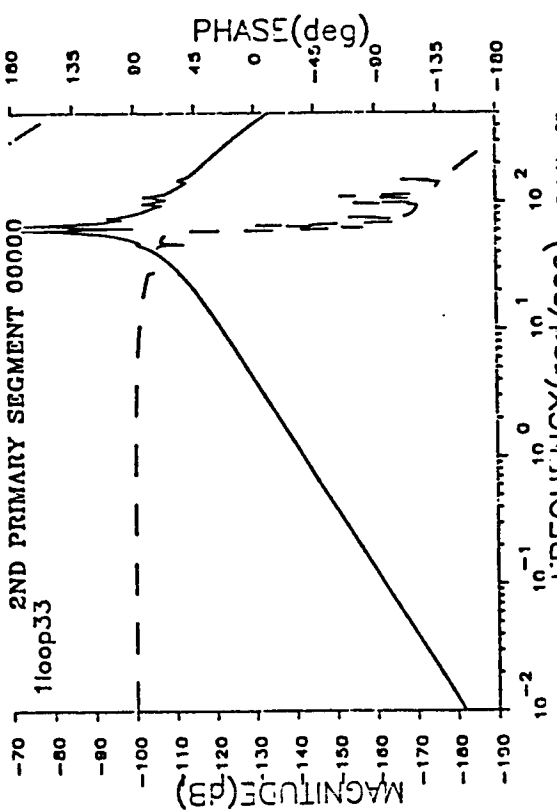


Figure 9. 2nd Primary Mirror Rate (rad/sec)/2nd Primary Mirror Applied Torque (N-m) all Feedback Paths Open.

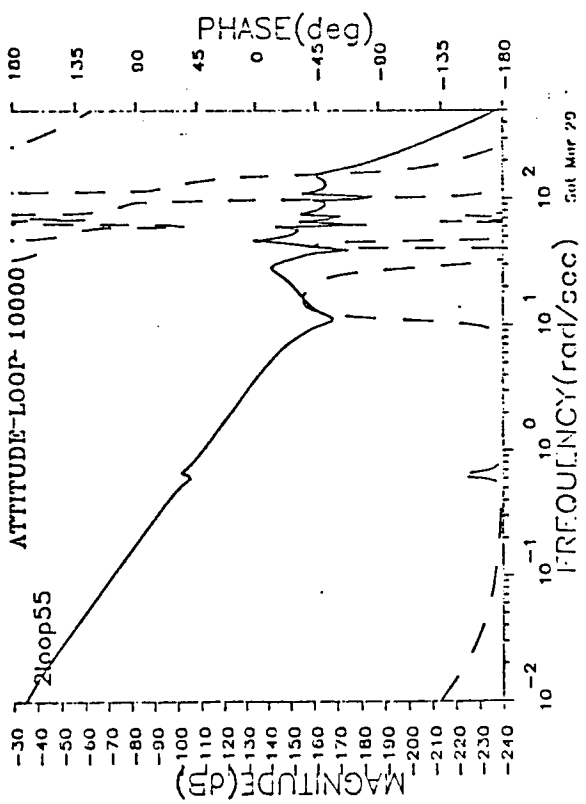


Figure 11. Tilt Angle (rad)/Gimbal Point Torque (N-m),
Secondary Mirror Loop Closed.

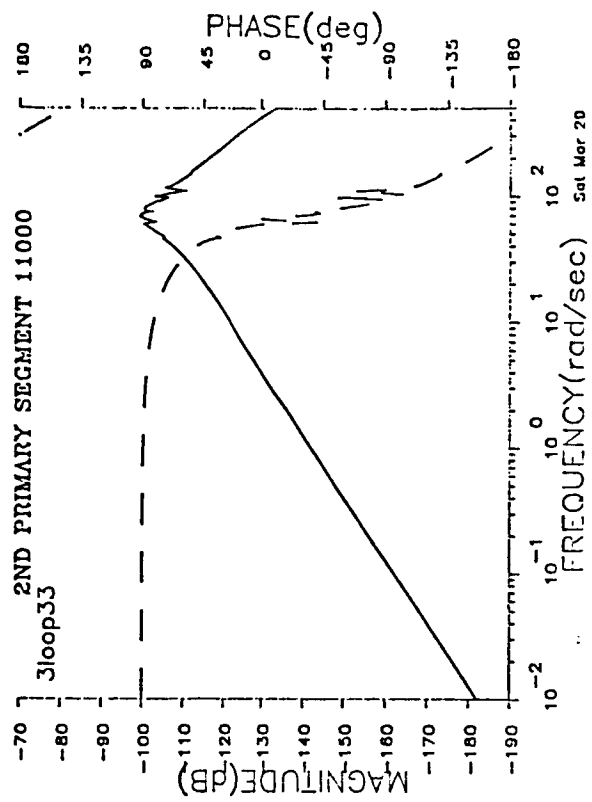


Figure 12. 2nd Primary Mirror Rate (rad/sec)/2nd Primary Mirror Applied Torque (N-m), and 1st PM Loops Closed.

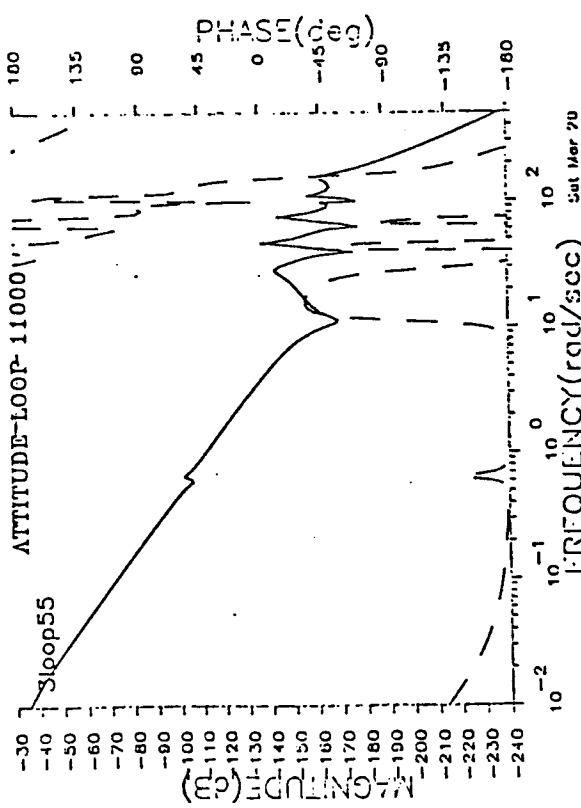


Figure 13. Tilt Angle (rad)/Gimbal Point Torque (N-m),
SM and 1st PM Loops Closed.

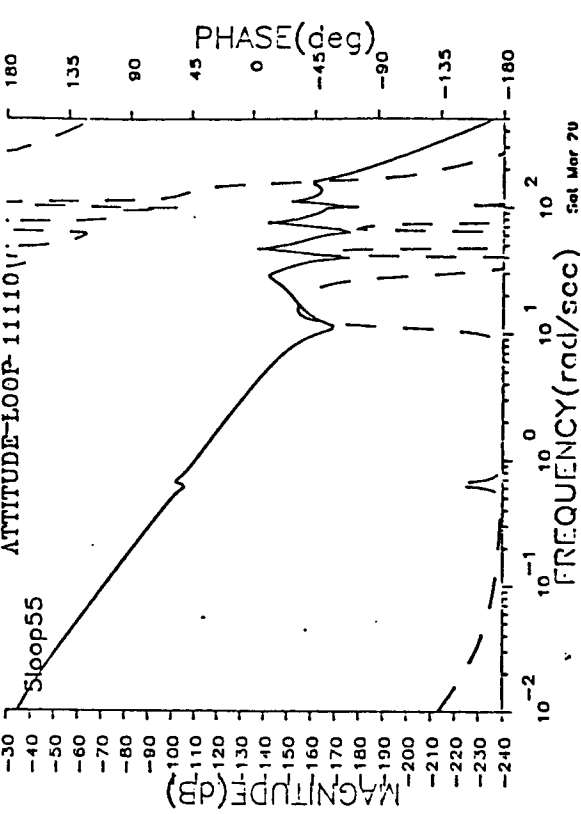


Figure 14. Tilt Angle (rad)/Gimbal Point Torque (N-m),
All Mirror Rate Loops Closed.

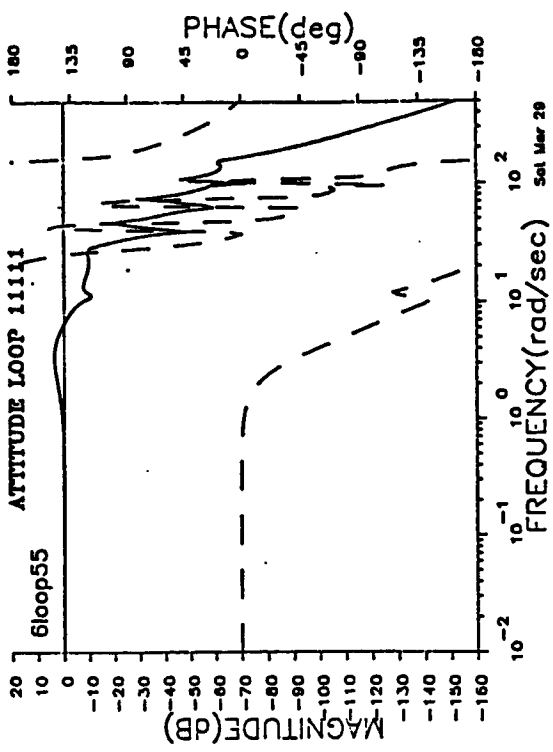


Figure 16. Tilt Angle (rad)/Gimbal Point Torque (N-m)
All Loops Closed.

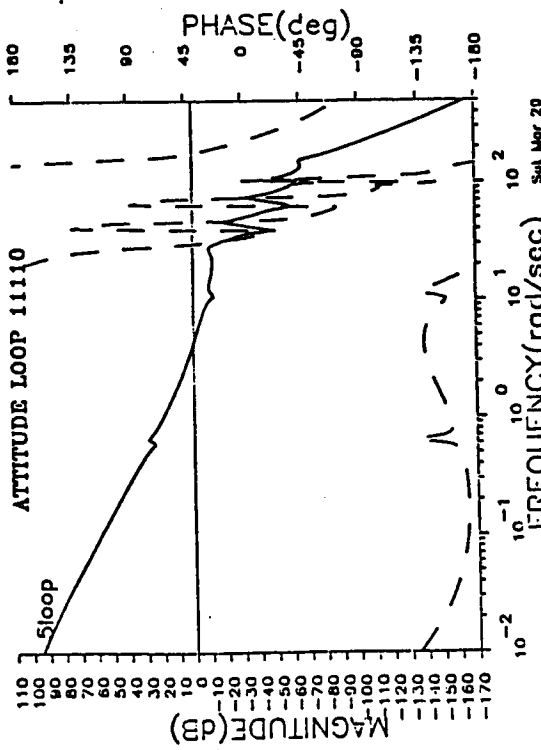


Figure 15. Tilt Angle (rad)/Gimbal Point Torque (N-m)
All Mirror Rate Loops Closed. $D_2(z)$ Included.

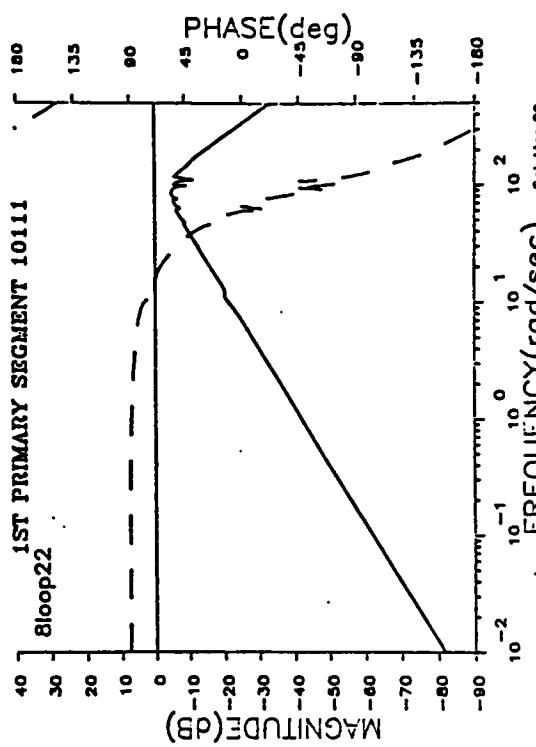


Figure 16. 1st Primary Mirror Rate (rad/sec)/1st Primary
Mirror Applied Torque (N-m), 1st Primary Loop
Open.

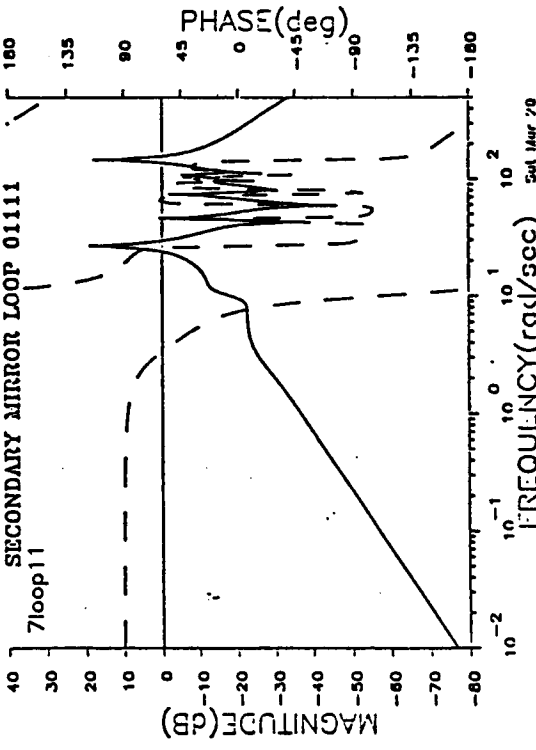


Figure 17. Secondary Mirror Rate (rad/sec)/Secondary Mirror
Applied Torque (N-m), SM Loop Open.

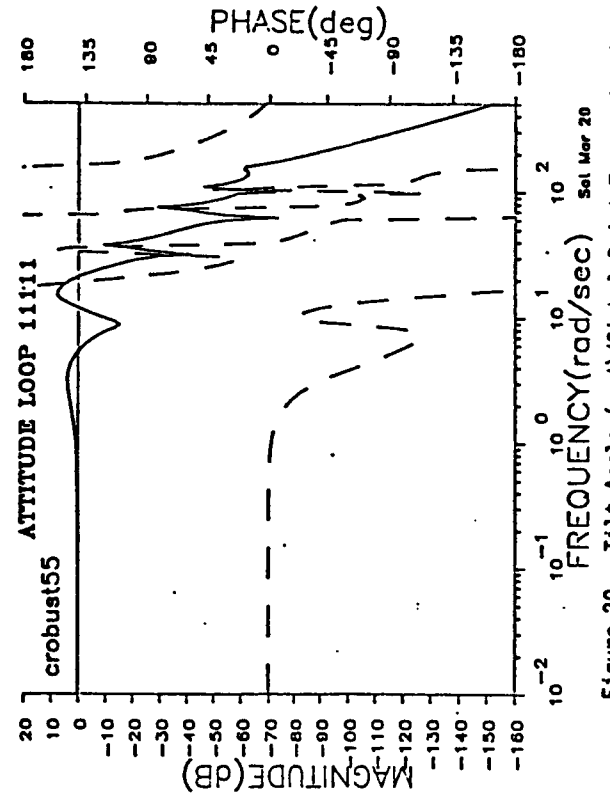


Figure 18. ATTITUDE LOOP 11111
robust55

FREQUENCY (rad/sec)

PHASE(deg)

MAGNITUDE (dB)

Sat Mar 20

All Loops Closed. First 2 Modes Reduced in Frequency by 20%.

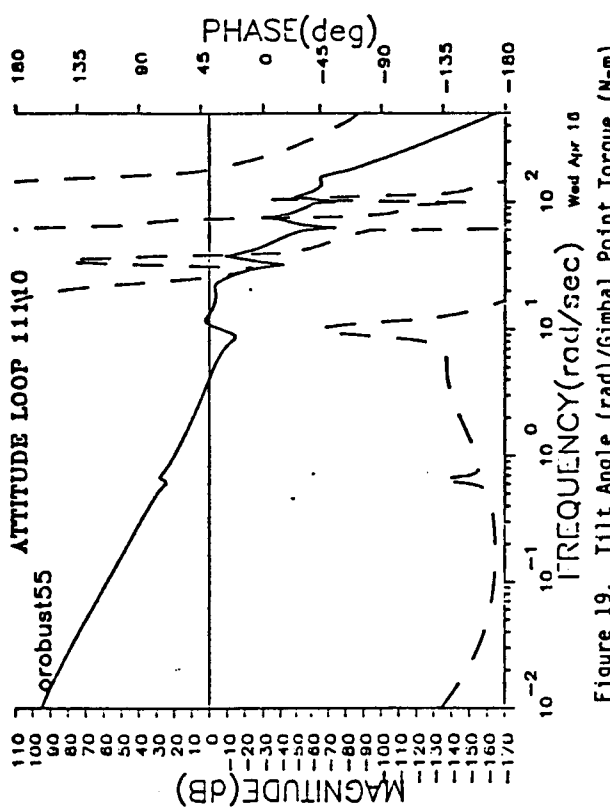


Figure 19. ATTITUDE LOOP 11110
robust55

FREQUENCY (rad/sec)

PHASE(deg)

MAGNITUDE (dB)

Wed Apr 10

Tilt Angle (rad)/Gimbal Point Torque (N-m)
Tilt Loop Open First 2 Modes Reduced in Frequency by 20%.

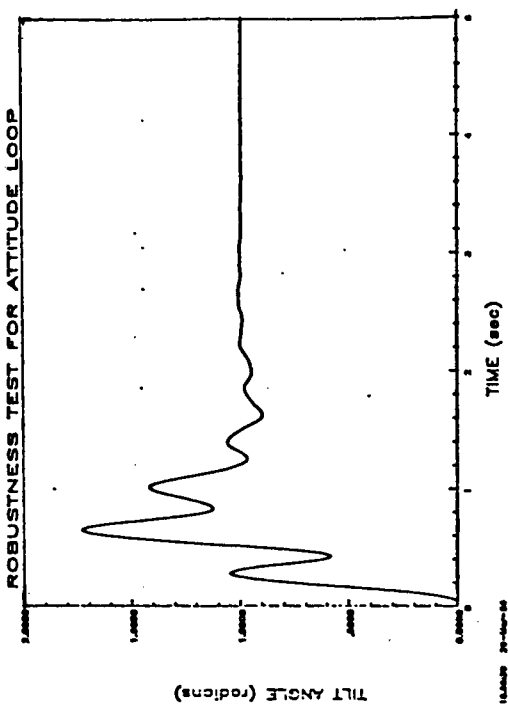


Figure 20. ROBUSTNESS TEST FOR ATTITUDE LOOP

TILT ANGLE (radians)

FREQUENCY (rad/sec)

PHASE(deg)

MAGNITUDE (dB)

Sat Mar 20

Tilt Angle (rad)/Gimbal Point Torque (N-m)
All Loops Closed. First 2 Modes Reduced in Frequency by 20%.

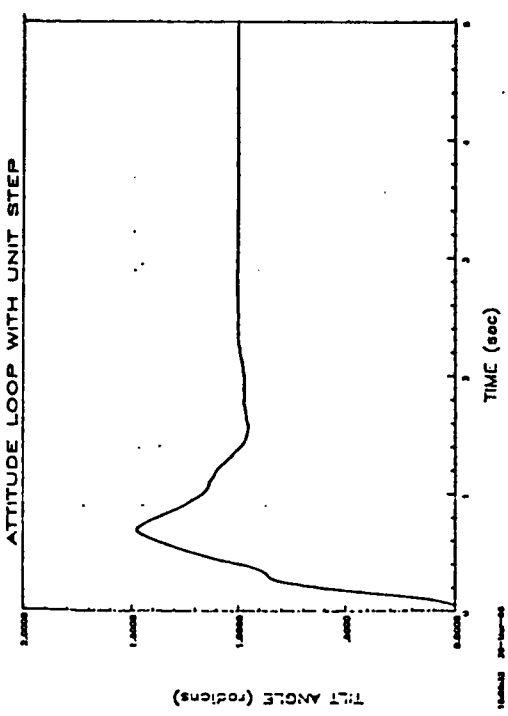


Figure 21. ATTITUDE LOOP WITH UNIT STEP

TILT ANGLE (radians)

TIME (sec)

ATTITUDE LOOP WITH UNIT STEP

Figure 22. TILT ANGLE RESPONSE TO A UNIT STEP COMMAND
Input with the First 2 Modes Reduced in Frequency by 20%.

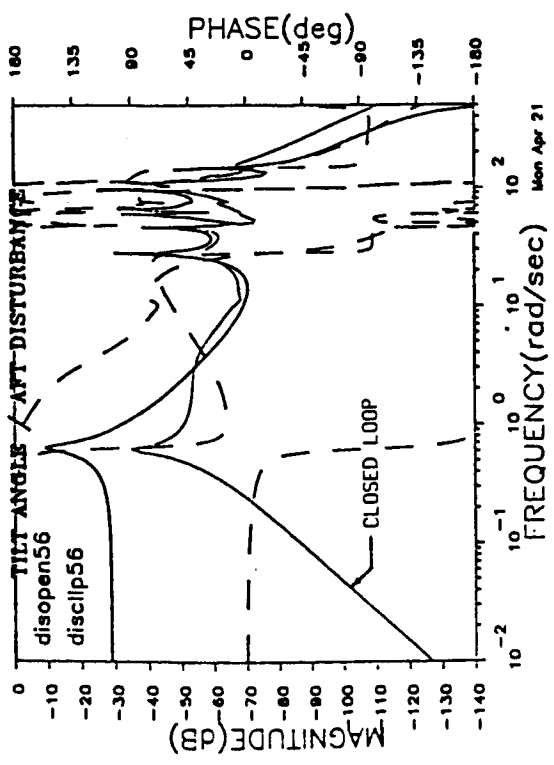


Figure 23 Tilt Angle (Rad)/AFT Disturbance Displacement
Open Loop and with all Loops Closed.

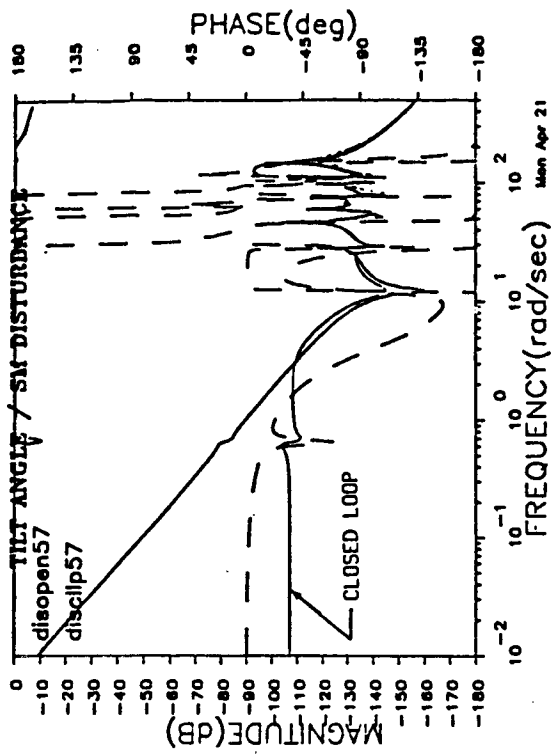


Figure 24 Tilt Angle (Rad)/SM Coolant Disturbance, Open Loop
and with all Loops Closed.

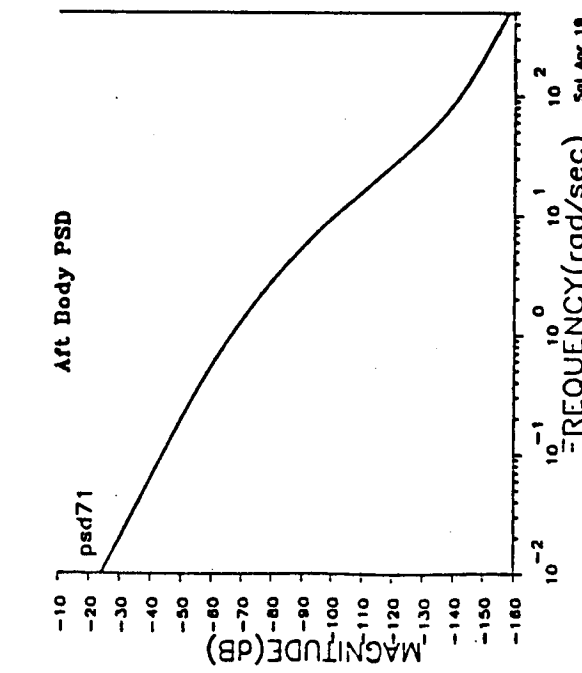


Figure 25 Aft Body Disturbance PSD dB=10 Log₁₀ (Mag)

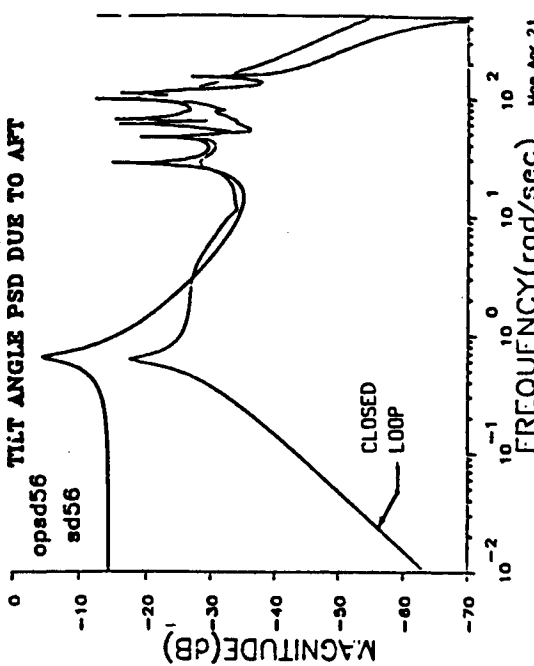


Figure 26 Tilt Angle PSD Due to Aft Body Disturbance, Open Loop
and with all Loops Closed dB=10 Log₁₀ (Mag).

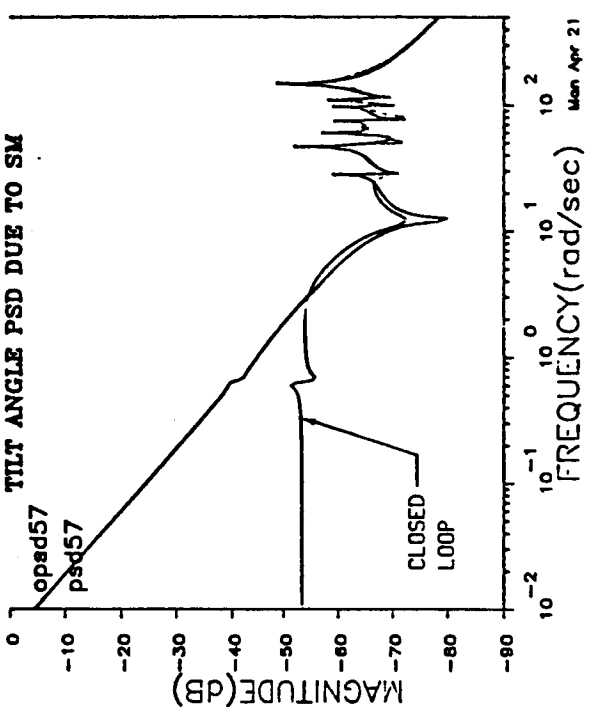


Figure 28 Tilt Angle PSD Due to SM Disturbance, Open Loop
and with all loops Closed $d\theta=10 \log_{10}$ (Mag).

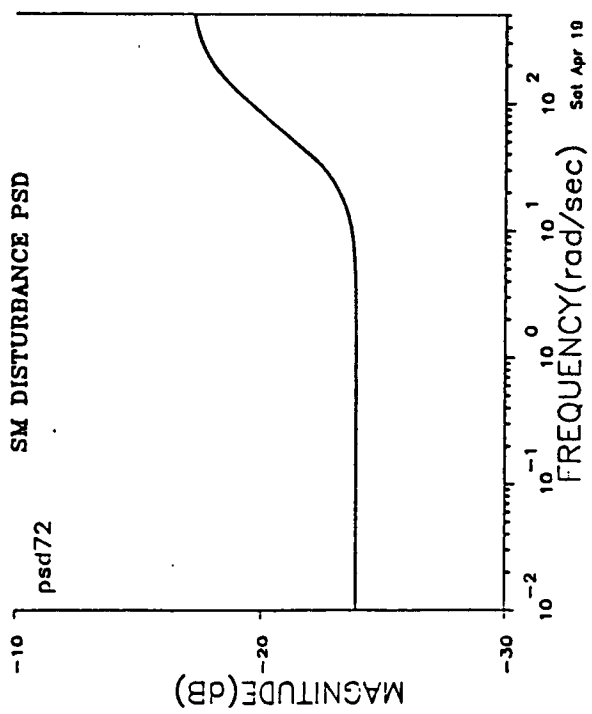


Figure 27 SM Coolant Flow Disturbance PSD $d\theta=10 \log_{10}$ (Mag).

Conclusion

In this paper the 1-CAT technique for designing multivariable control systems has been presented. The 1-CAT approach, within itself, does not dictate any particular design domain, although in the work presented here, frequency response techniques have been emphasized. Frequency domain techniques were selected in order that large order systems could be handled as easily as low order systems. In particular, after the frequency responses describing the plant are generated, system order is completely transparent in the 1CAT approach. The salient features of 1-CAT are as follows:

1. Provided the system is stabilizable, 1-CAT will produce a closed loop stable system.
2. The overall controller is relatively simple in comparison to those generated by modern control techniques, which typically produce controllers on the same order as the system model used.
3. By designing for a specified amount of relative stability and using phase stabilization of significant modes,⁵ robustness is an inherent part of the design.
4. 1-CAT is a straightforward, step-by-step procedure.

The 1-CAT approach was illustrated by designing a tilt angle control system for a planar model of the SBL. Although the design was for a single axis of the SBL, this is not a limitation of the 1-CAT technique. Design for a multiple axis model could have been done in a similar straightforward manner. A three axis design would be achieved by first designing all of the rate loops and then designing the position loops.

This paper has shown that the 1-CAT approach is a viable candidate for designing controllers for multiple input, multiple output systems. 1-CAT

assures a stable system. Since 1-CAT is straightforward, it appears feasible that it could be used as the basis of a self-tuning control algorithm. It is also feasible that 1-CAT could provide a baseline design that could then be optimized by other design approaches, e.g., a modified MIMO CIP,⁶ in order to maximize disturbance rejection while maintaining reasonable stability and robustness.

References

1. "ACOSS Five (Active Control of Space Structures) Phase II," Lockheed Missiles and Space Company, Inc., Sponsored by Defense Advanced Research Projects Agency, Report No. RADC-TR-82-21, March 1982.
2. "ACOSS Eight (Active Control of Space Structures) Phase II," TRW, Sponsored by Defense Advanced Research Projects Agency, Report No. RADC-TR-81-242, September 1981.
3. "ACOSS Fourteen (Active Control of Space Structures)," TRW, Sponsored by Defense Advanced Research Projects Agency, Contract No. F30602-81-0194, November 1982.
4. "ACOSS One (Active Control of Space Structures) Phase I," General Dynamics, Sponsored by Defense Advanced Research Projects Agency, Report No. RADC-TR-80-79, March 1980.
5. J. R. Mitchell, H. Eugene Worley, and Sherman M. Seltzer, "Digital Control System Design for a Precision Pointing System," Annual Rocky Mountain Guidance and Control Conference, Keystone, Colorado, February 5-9, 1983.
6. L. L. Gresham, J. R. Mitchell, and W. L. McDaniel, Jr., "A Multivariable Control System Design Algorithm," AIAA Journal of Guidance and Control, Vol. 3, No. 4, July August 1980.

Acknowledgement

The results presented here were used to support contract number F29601-83-C-0031, for the Air Force Weapons Laboratory, Kirtland AFB, New Mexico.